# RECENT PERSPECTIVES ON AXION COSMOLOGY

R.A. Battye
*Theoretical Physics Group, Blackett Laboratory, Imperial College*
*Prince Consort Road, London, SW7 2BZ, U.K.*

E.P.S. Shellard
*Department of Applied Mathematics and Theoretical Physics*
*University of Cambridge*
*Silver Street, Cambridge, CB3 9EW, U.K.*

We review current cosmological constraints on the axion. We describe the basic mechanisms by which axions are created in the early universe, focussing on the standard thermal scenario where the dominant process is through axion radiation by a string network. A dark matter axion in this case would have a mass $m_{\rm a} \sim 100\,\mu$eV, with specified large uncertainties. This cosmological lower bound leaves a viable window for the axion below the astrophysical upper limit, $m_{\rm a} \lesssim$ 1–10 meV. We also discuss alternative axion cosmologies which allow a much wider, but indefinite, mass range.

## 1 Introduction

Ever since the early 1980's, the axion has consistently remained one of the most popular dark matter candidates. Unlike many other more exotic particles, the axion's existence depends only on a minimal extension of the standard model[1,2] which also solves one of its key difficulties—the strong CP problem of QCD. In the standard thermal scenario for the early universe, cosmic axions are created by a variety of mechanisms ranging from 'quiescent' production of zero momentum axions when their mass 'switches on' at $t \approx 10^{-6}$ seconds[3] through to 'topological' production by the violent radiative decay of a network of axion strings formed at about $t = 10^{-25}$ seconds[4]. Originally, the role of axion strings was overlooked and calculations of the present axion density just from 'quiescent' mechanisms suggested a very light mass near $m_a \approx 5\,\mu$eV, that is, if the axion were to solve the dark matter problem[3]. However, it was soon recognized that axion strings provide the dominant cosmological contribution[4,5], and subsequent calculations[6] showed that a heavier mass range was appropriate $m_a \sim 100\,\mu$eV, though with additional uncertainties given the difficulty of these nonlinear calculations. Astrophysical constraints on the axion mass suggest that it must be less than about 1–10 meV, so the allowable axion parameter window is viable, though relatively narrow.

The present large-scale axion search experiment[7] is looking near the original mass range, $m_a \sim$ 1–10 $\mu$eV, for a variety of historical and technological

reasons. Such an axion is by no means excluded in some alternative scenarios which we shall also discuss. However, this paper will focus on the 'standard thermal scenario' which provides strong motivation for an expanded quest in search of a slightly heavier axion—an experiment that may become technically feasible in the not-too-distant future.

### *1.1 The origin of the axion*

The standard model of particle physics, based around the Weinberg-Salam model for electroweak interactions and QCD for strong interactions, has one significant flaw—the strong CP problem: non-perturbative effects of instantons add an extra term to the perturbative Lagrangian and the coefficient of this term, denoted $\bar{\theta}$, governs the level of CP violation in QCD. The absence of any such violation in all observed strong interactions imposes a constraint on $\bar{\theta}$, the most stringent being $\bar{\theta} < 10^{-10}$ due to the absence of a neutron electric dipole moment[8]. Since the value of $\bar{\theta}$ is effectively arbitrary, one is left with a severe fine tuning problem.

The elegant solution of Peccei and Quinn[1] is to allow $\theta$ to become a dynamical field which relaxes toward the CP conserving value $\bar{\theta} = 0$ [a], by the spontaneous breaking of a $U(1)$-symmetry. The resulting particle, known as the axion[2], has couplings to ordinary matter which are proportional to $f_{\rm a}^{-1}$ and acquires a mass $m_{\rm a}$ also proportional to $f_{\rm a}^{-1}$ at the QCD phase transition. Initially, it was supposed that the Peccei-Quinn scale was close to the electroweak phase transition $f_{\rm a} \sim T_{\rm EW}$, but an exhaustive search of accelerator data ruled this possibility out, implying $f_{\rm a} \gtrsim 10^7 {\rm GeV}$. However, the ensuing disappointment was short-lived because there is no phenomenological reason why the Peccei-Quinn scale $f_{\rm a}$ could not be much higher, even up to grand-unification scales. Thus, the 'invisible' axion was born, an extremely light particle with almost undetectably weak couplings of order $f_{\rm a}^{-1}$.

### *1.2 Astrophysical constraints on the axion*

Accelerator limits on the new 'invisible' axion were soon superseded by astrophysical calculations of cooling rates of large stars, such as red giants. Axions, being weakly coupled, escape from the whole volume of a star and, in certain parameter ranges, this can exceed the usual heat loss mechanisms through convection and other surface effects. The oft-quoted red giant constraint is $f_{\rm a} \gtrsim 10^9 {\rm GeV}$ (or $m_{\rm a} \lesssim 6\,{\rm meV}$)[10]. More stringent constraints on $f_{\rm a}$,

[a] In fact, $\bar{\theta} \neq 0$, since there are some CP violating weak interactions, and it has been shown that $\bar{\theta} > 10^{-14}$ in the standard model[9], although this is highly model dependent.

however, were thought to be imposed by neutrino emissions from supernova 1987a, providing the limit, $f_{\rm a} \gtrsim 10^{10}$GeV, which corresponds to a mass bound $m_{\rm a} \lesssim 0.6\,{\rm meV}$[11]. This 'conventional' wisdom has been questioned by Raffelt *et al.* who performed a detailed re-examination of these astrophysical calculations. They suggest that one cannot impose a meaningful constraint from SN1987a, since there is insufficient data, and, moreover, that the constraint from red giants is weaker than previously thought, $f_{\rm a} \gtrsim 5 \times 10^{8}$GeV (or $m_{\rm a} \lesssim 10\,{\rm meV}$)[12]. More recent work endeavours to answer some of these criticisms and reasserts a somewhat weaker bound from SN1987a, $f_{\rm a} \gtrsim 10^{9}$GeV (or $m_{\rm a} \lesssim 6\,{\rm meV}$), though this can be an order of magnitude tighter depending on the axion model parameters[13]. This topic lies outside the scope of the present discussion, so more general reviews should be consulted[14].

### *1.3 Cosmological axions: 'quiescent' vs. 'topological' production*

The weak coupling to ordinary matter and the substantial redshifting between the Peccei-Quinn and QCD phase transitions make the axion an ideal cold dark matter candidate. The earliest estimates of the cosmological axion density[28,3] assumed 'quiescent' production, that is, axions were created through coherent oscillations about the minimum of the Peccei-Quinn potential when the axion mass 'switched on' at $T \sim \Lambda_{\rm QCD}$. A recent estimate of the relative contribution of these zero momentum axions is

$$\Omega_{\rm a,h} \approx 0.9 h^{-2} \Delta \left( \frac{f_{\rm a}}{10^{12}{\rm GeV}} \right)^{1.18} \bar{\theta}_i^2 \,, \tag{1}$$

where $\Delta \sim 1$ accounts for the uncertainties in the QCD phase transition (discussed later)[15]. Assuming an ill-defined 'average' value of the axion field $\langle \bar{\theta}_i^2 \rangle = \pi^2/3$, implies a constraint $f_{\rm a} \lesssim 10^{12}{\rm GeV}\,, m_{\rm a} \gtrsim 5\mu{\rm eV}$ when compared to the closure density of a flat universe $\Omega = 1$. As we have emphasised already, this estimate ignores much stronger topological effects arising at the Peccei-Quinn phase transition, that is, the inevitable creation of an axion string network.

If we suppose that we live in a universe that underwent an inflationary phase in the early universe, then there are two basic scenarios for cosmological axion production. These depend on the relationship between the inflationary reheat temperature $T_{\rm reh}$ and the string-forming phase transition temperature $T_{\rm PQ} \sim f_{\rm a}$:

1. If the reheat temperature $T_{\rm reh}$ is sufficient to restore the Peccei-Quinn symmetry $T_{\rm reh} > f_{\rm a}$, then a network of global or axion strings will form

by the Kibble mechanism. This is the usual thermal scenario commonly assumed in most of the axion literature. Here, we *can* predict the mass of the axion if it constitutes the main dark matter component of the universe.

2. Alternatively, if $T_{\rm reh} < f_{\rm a}$, then any strings which may have been formed before the inflationary epoch would be diluted by the subsequent rapid exponential expansion with which it is associated. In this case, we *cannot*, in principle, make a definite prediction about the axion mass on cosmological grounds.

It is important to elaborate this 'predictive' distinction because, in simple inflationary scenarios with $T_{\rm reh} < f_{\rm a}$, the estimate (1) will still apply and a mass prediction appears to be meaningful. However, $\theta_{\rm i}$ is homogeneous over an entire inflationary domain, certainly exceeding the present horizon, and it is set to a fixed, but arbitrary, value. By (1), this *unknown* value of $\theta_{\rm i}$ in our domain very precisely defines the value of $m_{\rm a}$ required for the axion to be the dark matter—or vice versa. Either way, we have some sort of tuning re-emerging, which is not particularly consistent with the original motivation for the axion[b]. Nevertheless, in section 4 we discuss this scenario, which gives a wide range of possible axion masses, along with other 'non-standard' scenarios. We also note that topological defects may have formed during inflation[17] or that they may have been created at the end of inflation during a phase transition[18], effectively removing this new fine-tuning problem by returning us to the first case (i). For this reason, we describe the axion string picture as the 'standard thermal scenario'; it is essentially the original axion cosmology understood more completely.

If a string network does form, then its decay into axions will provide the dominant contribution to the overall axion density[4,5,19], since the topological effects involved are much stronger than the coherent zero-momentum contributions of (1). In this scenario the axion field $\theta$ is assigned different values at every point in space by the topological requirement that $\theta$ changes by $2\pi$ around each string. This removes the possibility of any kind of fine-tuning of $\theta_{\rm i}$, since the distribution of strings is dictated by the dynamics of the phase transition. However, the spectrum of the radiation from these strings has been the subject of much debate[20,4,21,22,5] because it dictates the magnitude of this

[b]Linde suggests that in the infinite 'manifold' of a chaotic inflationary model, all values of $\theta_{\rm i}$ will be realized, so this fine-tuning can be interpreted merely as a manifestation of the anthropic principle[16]; the axion-to-baryon ratio is set by $\theta_{\rm i}$ and humankind can only tolerate a narrow band of ratios! However, many find this form of 'explanation' decidedly unappealing.

contribution. Indeed, it appears that the over-production of axions by strings could almost close the allowed window of values for $f_{\rm a}$, given the lower bound provided by astrophysical effects.

In recent years, we have undertaken a thorough investigation of the string radiation spectrum, using both analytic and numerical techniques[23,24,19,25]. The findings were in broad agreement with the initial work of Davis *et al.*[20,4,5], but not with the work of Sikivie *et al*[21,22] which results in a weaker constraint. Taken at face value the earlier results of Davis *et al.* would eliminate the axion as a cold dark matter candidate in the standard scenario. However, although the underlying physics of the earlier work was correct, the model for string evolution on which it was based was too simplistic. Subsequent work has provided a more sophisticated picture of axion production by a string network which does leave an window open for the axion.

### *1.4 Overview*

In this article, we review the cosmological constraints on the axion, in particular, adding greater detail to an earlier letter on the axion string bound. We introduce a simple model for the evolution of a network of cosmic axion strings based on a 'one-scale' model. Using this model we calculate expressions for the contibution to the axion density from string loops and the long string network, exhibiting explicit parameter dependencies. By comparing to the closure density, we estimate the constraint on the Peccei-Quinn symmetry breaking scale $f_{\rm a}$ and the axion mass $m_{\rm a}$. In the standard scenario, we show that this contribution completely dominates the axion density from 'quiescent' zero-momentum production[3].

We note that there has been considerable controversy associated with the nature of axion string radiation and how this affects the resulting cosmological constraint. For this reason we provide an appendix discussing this topic in some detail. We present a tight mathematical argument, based on the low energy Kalb-Ramond action for axion strings, which demonstrates that radiation goes primarily into the lowest frequency modes available. This understanding is shown to be in quantitative agreement with high resolution numerical simulations of the full U(1) field equations even at moderately high energies. This establishes beyond reasonable doubt the efficacy of the Kalb-Ramond action for describing axion string dynamics, thus providing a firm basis for the cosmological calculations.

Finally, we discuss 'non-standard scenarios' including some of the broad array of inflationary variants and we also consider the possibility of axion dilution by entropy production due to the out-of-equilibrium decay of massive

particles. Our conclusions summarize the best current estimates of the cosmological constraint on the axion.

## 2 Axion string network evolution

The evolution of axion strings is qualitatively very similar to the evolution of local strings due to their dynamical correspondence—as demonstrated in the appendix. The additional long-range field, due to the coupling to the axion, acts primarily to renormalize the string tension and energy density,

$$\mu \approx 2\pi f_{\rm a}^2 \ln(t/\delta)\,, \tag{2}$$

where the string core width is $\delta \sim f_{\rm a}^{-1}$ and we assume the typical curvature radius of the strings at a time $t$ is $R \sim t$. Quantitatively, on small scales $\ell \ll t$, global strings are affected by enhanced radiation backreaction; typically in a cosmological context axion radiation will be three orders of magnitude stronger than the weak gravitational radiation produced by local strings. This difference will alter small-scale features such as string wiggliness and loop creation sizes, but not the more robust large-scale network properties. We comment further on the nature of string radiation in the next section.

All the pertinent events take place in the radiation era, so for definiteness we consider a flat ($\Omega = 1$) FRW model with

$$a \propto t^{1/2}\,, \quad \rho = \frac{3}{32\pi G t^2}\,, \quad n \approx 0.12\mathcal{N}T^3\,, \quad t \approx 0.3\mathcal{N}^{-1/2}\frac{m_{\rm pl}}{T^2}\,, \tag{3}$$

where $\rho$ is the energy density, $n$ is the particle number density, and $\mathcal{N}(T)$ is the effective number of massless degrees of freedom at the temperature $T$.

### *2.1 String network formation and the damped epoch*

The string-forming phase transition creates a tangled network permeating throughout the universe. The largest fraction (over 80%) of string makes up a random walk of long or 'infinite' strings, and a scale-invariant distribution of closed loops makes up the remainder. After formation, these strings experience a significant damping force due to the relatively high radiation background density. In the case of local strings, the dominant interaction is through Aharonov-Bohm type scattering. This frictional force will dominate the dynamics of the strings, until the Hubble damping force becomes larger. The temperature and time corresponding of this transition are given by

$$T_* \sim (G\mu)^{1/2}\eta\,, \quad t_* \sim (G\mu)^{-1}t_{\rm f}\,, \tag{4}$$

where $G = m_{\rm pl}^{-2}$ is Newton's constant, $\mu$ is the string energy per unit length, $\eta$ is the symmetry breaking scale and $t_{\rm f}$ is the time of formation.

There are no gauge fields present for global strings and therefore Aharonov-Bohm type scattering no longer pertains. In this case, one finds that Everett scattering is the dominant process, with a scattering cross-section[26]

$$\frac{d\sigma}{d\theta} = \frac{\pi}{4q[\log(\delta q)]^2}\,, \tag{5}$$

where $q \sim T$ is the momentum of the incident particle and $\delta \sim f_{\rm a}^{-1}$ is the width of the string.

As for local strings, the frictional force per unit string length can be estimated as

$$\mathbf{F} \sim n\sigma_{\rm t} v_T \Delta\mathbf{p}\,, \tag{6}$$

where $\sigma_t$ is the transport cross-section given by

$$\sigma_{\rm t} = \frac{\pi^2}{2q[\log(q\delta)]^2} \sim T^{-1}[\log(T\delta)]^{-2}\,, \tag{7}$$

$v_T \sim 1$ is the thermal velocity of the particles and $\Delta\mathbf{p} \sim -T\mathbf{v}$ is the average momentum transfer per collision where $T$ is the temperature.

By comparison to the Hubble damping force we find that the temperature at which frictional damping becomes negligible is given by

$$\frac{T_*}{[\log(T_*/f_{\rm a})]^2} \sim G\mu m_{\rm pl}\,. \tag{8}$$

This implies that strings oscillate relativistically and begin to radiate axions from the time,

$$t_* \sim 10^{-20}\left(\frac{f_{\rm a}}{10^{12}{\rm GeV}}\right)^{-4} {\rm sec}\,. \tag{9}$$

### *2.2 The scaling regime for string network evolution*

After the damped epoch, the strings are expected to evolve towards a scale-invariant regime by the formation of loops and subsequent emission of radiation. This scaling regime is likely to be achieved irrespective of the radiative mechanism, although the important parameters describing the network will be somewhat different.

The overall density of strings splits neatly into two distinct parts, the long strings with length $\ell > t$ and small closed loops with $\ell < t$,

$$\rho = \rho_\infty + \rho_L\,. \tag{10}$$

The exact length scale $l_c$, at which the distinction between long strings and loops is made is unimportant since large loops are rare, but it is normally assumed to be comparable to the horizon. However, this distinction is important since loops will be radiated away quickly, whereas long strings will remain until domain walls form close to the QCD phase transition.

If we ignore radiative effects, then the dynamics of the strings can be described by the Nambu action. The equations of motion for a string in an expanding background are

$$\ddot{\mathbf{X}} - \frac{1}{\epsilon}\left(\frac{\mathbf{X}'}{\epsilon}\right)' = -\frac{2\dot{a}}{a}(1-\dot{\mathbf{X}}^2)\dot{\mathbf{X}}\,, \quad \dot{\epsilon} = -\frac{2\dot{a}}{a}\epsilon\dot{\mathbf{X}}^2\,, \tag{11}$$

using the temporal transverse gauge, where the string coordinates are $X^\mu = (t, \mathbf{X})$, $\dot{\mathbf{X}}\cdot\mathbf{X}' = 0$ and $\epsilon^2 = \mathbf{X}'^2/(1-\dot{\mathbf{X}}^2)$. In this gauge, the string energy is given by

$$E = \mu_0 \int d\sigma\epsilon\,, \tag{12}$$

where $\sigma$ is a spacelike coordinate along the string. Differentiating this expression with respect to time and substituting in the expression for $\dot{\epsilon}$ from (11), one can obtain

$$\dot{E} = -2\langle v^2\rangle E\,, \quad \dot{\rho} = -2(1+\langle v^2\rangle)\rho\,, \tag{13}$$

where $\langle v^2\rangle$ is the average string velocity defined by

$$\langle v^2\rangle = \int d\sigma\epsilon\dot{\mathbf{X}}^2 \Big/ \int d\sigma\epsilon\,, \tag{14}$$

with $E = \rho V$ and $V \propto a^3$. In this model, $\langle v^2\rangle$ is an unknown constant to be determined for long strings, and $\langle v^2\rangle \approx 1/2$ for string loops. Therefore, excluding radiative effects and the formation of loops, the density of long strings and loops evolve independently according to

$$\dot{\rho}_\infty = -\frac{2\dot{a}}{a}\big(1+\langle v^2\rangle\big)\rho_\infty\,, \qquad \dot{\rho}_L = -\frac{3\dot{a}}{a}\rho_L\,. \tag{15}$$

The equations (15) do not take into account the loss of energy to loops. The rate of energy loss from the long string network into loops can be described in terms of a scale invariant production function $f(\ell/L)$ where $\ell$ is the loop size and $L$ is the characteristic length of the long string network. This function is defined so that $\mu f(\ell/L)d\ell/L$ gives the energy loss into loops of size $\ell$ to $\ell + d\ell$ per unit time per correlation volume $L^3$. The equations for the long string density and the loop density are

$$\dot{\rho}_\infty = -\frac{2\dot{a}}{a}\big(1+\langle v^2\rangle\big)\rho_\infty - \frac{c\rho_\infty}{L}\,, \qquad \dot{\rho}_L = -\frac{3\dot{a}}{a}\rho_L + \frac{g\mu}{L^4}f(\ell/L)\,, \tag{16}$$

where $g$ is a Lorentz factor and $c$ is measure of loop production rate given by

$$c\rho_\infty = \frac{\mu}{L^3}\int_0^{\ell_c} d\ell\, f(\ell/L)\,. \tag{17}$$

In order to investigate these equations, one can substitute $\rho_\infty = \mu\zeta/t^2$ and $L = \zeta^{-1/2}t$ into the equation for $\rho_\infty$. If $\zeta$ is constant, then we have that the density of long strings will scale like radiation or matter in their respective eras, and the evolution is self-similar that is, the large scale features of the string network will look the same at all times, except for a universal scaling proportional to the change in horizon size. Performing this substitution, one obtains

$$\frac{\dot{\zeta}}{\zeta} = \frac{1}{t}\left(2 - 2\beta\big(1 + \langle v^2\rangle\big) - c\zeta^{1/2}\right), \tag{18}$$

where the scale factor is given by $a(t) \propto t^\beta$. This equation has a stable fixed point solution for $\zeta$, corresponding to the scaling regime. Setting the right hand side of this equation to zero allows one to derive a relation between the loop production rate, the long string density and the average velocity of the long strings.

Using $a(t) \propto t^{1/2}$ in the radiation era, one can deduce that the loop production rate required to maintain scaling is $c = \zeta^{-1/2}\big(1 - \langle v^2\rangle\big)$. One can also solve the equation for the density of loops to give

$$\rho_L = \frac{g\mu\zeta^{5/4}}{(\ell t)^{3/2}}\int_{\zeta^{1/2}\ell/t}^{\infty} dx\sqrt{x}f(x)\,, \tag{19}$$

which can be approximated at late times by $\rho_L = \mu\nu(\ell t)^{-3/2}$ where

$$\nu = g\zeta^{5/4}\int_0^{\infty} dx\sqrt{x}f(x)\,. \tag{20}$$

Hence, the number density of loops in the interval $\ell$ to $\ell + d\ell$ defined as $\mu\ell\, n(\ell,t)\, d\ell = \rho_L(\ell,t)d\ell$ is given by

$$n(\ell,t) = \frac{\nu}{\ell^{5/2}t^{3/2}}\,. \tag{21}$$

At this stage we have to make an assumption as to the form of the loop production function $f(x)$. One of the basic philosophies behind the scaling regime is that all the properties of the string network are constant with respect to the horizon. Therefore, a sensible assumption seems to be that the

loop production function is peaked at some constant fraction of the horizon. Mathematically, we treat this as a delta function

$$f(x) = c\delta(x - \alpha\zeta^{1/2})\,, \tag{22}$$

and finally one obtains

$$\nu = gc\alpha^{1/2}\zeta^{3/2} = g\alpha^{1/2}\zeta\big(1 - \langle v^2\rangle\big)\,. \tag{23}$$

These expressions do not take into account the effects of radiation on the strings loops which we discuss in the next section. However, this can be achieved simply using a linear decay of string loop energy given by $\ell = \ell_0 - \kappa(t - t_0)$. Using $\ell_0 = \alpha t_0$, one can deduce that

$$\ell_0 = \frac{\ell + \Gamma G\mu t}{1 + \Gamma G\mu/\alpha}\,. \tag{24}$$

Making the substitution $\ell \to l_0$, that is, $n(\ell_0, t)d\ell_0 \to n(\ell, t)d\ell$, the number density of loops in the radiation, taking into account the decay of loop length, is given by

$$n(\ell, t) = \frac{\nu}{(\ell + \kappa t)^{5/2} t^{3/2}}\,, \tag{25}$$

with $\nu$ redefined to be

$$\nu = \big(1 + \kappa/\alpha\big)^{3/2} g\alpha^{1/2}\zeta\big(1 - \langle v^2\rangle\big)\,. \tag{26}$$

All these parameters, but for the loop size $\alpha$, can be reliably estimated from high resolution simulations of local strings[27,28] (for example, $\zeta \approx 13$).

### *2.3 Axion mass 'switch on' and domain walls*

Near the QCD phase transition the axion acquires a mass and network evolution alters dramatically because domain walls form[30], with each string becoming attached to a wall[31]. 'Soft' instanton calculations give the initially temperature dependent mass[2,15]

$$m_{\rm a}(T) = (0.1 \pm 0.03)\bar{m}_{\rm a}\left(\frac{f_{\rm a}}{10^{12}{\rm GeV}}\right)^{-1}\left(\frac{\Lambda_{\rm QCD}}{T}\right)^{3.7\pm0.1}\,, \tag{27}$$

which achieves its maximum value for $T >> \Lambda_{\rm QCD}$ at

$$m_{\rm a} = \bar{m}_{\rm a}\left(\frac{f_{\rm a}}{10^{12}{\rm GeV}}\right)^{-1}\,. \tag{28}$$

This mass only becomes significant when the Compton wavelength falls inside the horizon, that is, $m(\tilde{t})\tilde{t} \sim 0.75$ at the time

$$\tilde{t} \sim 10.8 \times 10^{-7} \Delta^2 \left( \frac{f_{\rm a}}{10^{12}{\rm GeV}} \right)^{0.36} \left( \frac{\bar{m}_{\rm a}}{6 \times 10^{-6}{\rm eV}} \right)^{-2} \left( \frac{\mathcal{N}_{\rm QCD}}{60} \right)^{0.5} {\rm sec}\,, \quad (29)$$

where $\Delta$ is a constant of order unity which quantifies parameter uncertainties at the QCD phase transition [c],

$$\Delta = 10^{\pm 0.5} \left( \frac{\bar{m}_{\rm a}}{6 \times 10^{-6}{\rm eV}} \right)^{0.82} \left( \frac{\Lambda_{\rm QCD}}{200{\rm MeV}} \right)^{-0.65} \left( \frac{\mathcal{N}_{\rm QCD}}{60} \right)^{-0.41} . \quad (30)$$

Large field variations around the strings collapse into localized domain walls at $\tilde{t}$. Subsequently, these domain walls begin to dominate over the string dynamics when the force from the surface tension becomes comparable to the tension due to the typical string curvature $\sigma \sim \mu/t$,

$$t_{\rm w} \sim 1.7 \times 10^{-6} \Delta^2 \left( \frac{f_{\rm a}}{10^{12}{\rm GeV}} \right)^{0.36} \left( \frac{\bar{m}_{\rm a}}{6 \times 10^{-6}{\rm eV}} \right)^{-2} \left( \frac{\mathcal{N}_{\rm QCD}}{60} \right)^{0.5} {\rm sec}\,. \quad (31)$$

The demise of the hybrid string–wall network proceeds rapidly[31], as demonstrated numerically[32,33,34]. The strings frequently intersect and intercommute with the walls, effectively 'slicing up' the network into small oscillating walls bounded by string loops. Multiple self-intersections will reduce these pieces in size until the strings dominate the dynamics again and decay continues through axion emission.

## 3 The nature of axion string radiation

Axion strings oscillate relativistically and radiate their energy primarily into axions; this is the preferred channel because the string coupling to the axion is much stronger than, say, gravitational radiation. The axion string is a global string with a long-range Goldstone boson field in which most of its energy resides, as the logarithm in (2) indicates. With $f_{\rm a} \sim 10^{10}\,{\rm GeV}$ this effective renormalization is about $\log(t/\delta) \approx 70$, but the apparent 'non-locality' of a global string is more imagined than real. To illustrate this point, consider surrounding a straight axion string with a narrow tube of radius $R \sim t/100$; this tube would contain 95% of the string's energy while only enclosing 0.03% of

[c] Note that to calculate $\tilde{t}$, we assume an effective number of massless degrees of freedom $\mathcal{N}$ in an epoch when its actual value is falling. However, it should be possible to use an averaged value throughout this epoch.

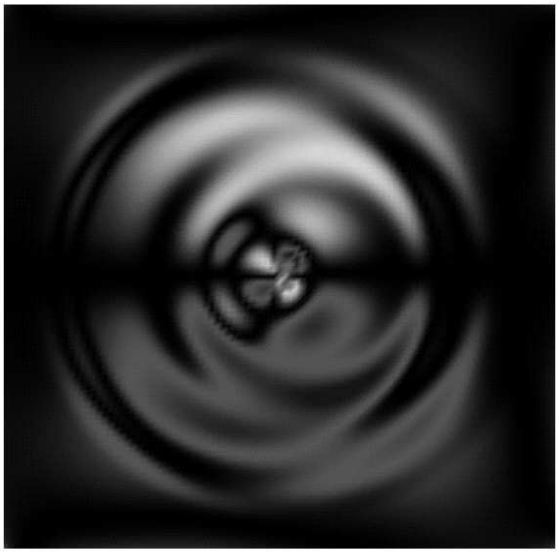

Figure 1: Axion radiation from an oscillating periodic string configuration in a three-dimensional field theory simulation. In this perpendicular cross-section, the string oscillates horizontally. Note the dominance of $n = 2$ quadrupole radiation.

the available volume. Nevertheless, the understanding of global or axion string dynamics has some heuristic pitfalls and, in the past, there was considerable debate on the subject. In order to assure the reader of the veracity of the conclusions that follow on this key issue, an appendix is provided summarizing more recent literature on the subject.

On cosmological scales, as we have stated already, the basic fact is that the axion string essentially behaves like a local cosmic string, but with stronger radiation damping. The radiation power arising from an oscillating string loop is independent of it size. This scale-invariant power is given by

$$P = \Gamma_{\rm a} f_{\rm a}^2 \equiv \kappa\mu, \tag{32}$$

where $\Gamma_{\rm a} \approx 65$ has been found from numerical simulations and $\kappa$ essentially defines the radiation backreaction scale. This radiation power loss leads to the linear decay of the loop size with time,

$$\ell = \ell_{\rm i} - \kappa(t - t_{\rm i})\,. \tag{33}$$

Any loop will disappear into axions after about 10–20 oscillations.

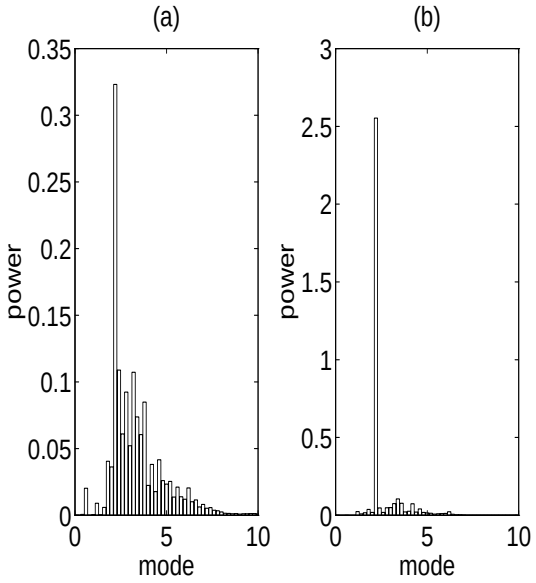


Figure 2: Power spectrum of axion radiation from an oscillating periodic string (as in fig. 2). Here, the initial string configuration has a sharp 'kink', but the initial high frequency radiation (a), rapidly gives way at later times to the dominant $n = 2$ quadrupole radiation (b). This spectral evolution demonstrates the effect of radiative backreaction.

The radiation spectrum into which the loops decay is dominated by the lowest available frequencies, that is, the lowest harmonic wavelengths proportional to the loop size $\ell$. If we decompose the loop radiation spectrum into the power in each harmonic $P_n$ then we expect a power law fall-off at large $n$, that is,

$$P = \sum_n P_n, \qquad Pn \propto n^{-q} \;\; (n >> 1)\,, \quad \text{with} \;\; q \geq 4/3\,. \tag{34}$$

For typical loops, the spectral index $q$ is expected to be greater than $4/3$ because of radiative backreaction effects. The fact that the spectrum is dominated by the lowest harmonics can be seen in some results from numerical simulations of axion strings illustrated in figs. 1–2. For this particular axion string configuration the quadrupole ($n = 2$) is most prominent, as shown quantitatively in fig. 2 with a power spectrum analysis.

The key uncertainty in cosmic axion calculations is the scale-invariant size $\ell = \alpha t$ at which loops are created by the string network. The parameter $\alpha$ is determined by radiative backreaction effects on the string network and, since

the backreaction scale is set by $\kappa$ in (32), most authors anticipate $\alpha \approx \kappa$. However, smaller values are not necessarily excluded[23], so here we consider the range $0.1 \lesssim \alpha/\kappa \lesssim 1.0$, and this key parameter will appear in subsequent axion bounds. The above facts are all we need to know to calculate the cosmic axion abundance.

## 4 The axion density in the standard thermal scenario

Given the loop distribution (25), we can calculate the energy density of emitted axions. The radiation spectrum from a loop of length $\ell$, averaged over various loop configurations, is given by

$$\frac{dP_\ell(\omega)}{d\omega} = f_{\rm a}^2 \ell \, g(\ell\omega) \,, \tag{35}$$

where the spectral function $g(x)$—a continuum limit of (34)—is normalised by

$$\int_0^\infty g(x) dx = \Gamma_{\rm a} \,, \tag{36}$$

and $\Gamma_{\rm a}$ is defined in (32). We shall assume that loops are at rest, because any initial velocity will be redshifted and the net error when averaged isotropically over all loops should be relatively small.

The energy density of massless axions emitted at time $t_1$ in an interval $dt_1$ with frequencies from $\omega_1$ to $\omega_1 + d\omega_1$ is

$$d\rho_{\rm a}(t_1) = dt_1 d\omega_1 f_{\rm a}^2 \int_0^\infty d\ell \, n(\ell, t_1) \ell \, g(\ell\omega) \,. \tag{37}$$

Assuming $\mathcal{N}$ constant, the spectral density can be calculated by integrating over $t_1 < t$, taking into account the redshifting of both the frequency, $\omega = a(t_1)/a(t)\omega_1$, and the energy density, $\rho_{\rm a} \propto a^{-4}$. Neglecting the slow logarithmic dependence of the backreaction scale $\kappa$, we have

$$\frac{d\rho_{\rm a}}{d\omega}(t) = \frac{f_{\rm a}^2}{t^{3/2}} \int_{t_*}^t dt_1 \int_0^{\alpha t_1} d\ell \, \frac{\nu\ell}{(l + \kappa t_1)^{5/2}} \, g\left[ (t/t_1)^{1/2} \, \omega\ell \right] . \tag{38}$$

Under the substitution $x = \ell/t_1$ , $z = \omega x (t t_1)^{1/2}$, the range of integration is transformed and (38) becomes[35]

$$\frac{d\rho_{\rm a}}{d\omega}(t) = \frac{4 f_{\rm a}^2 \nu}{3\omega\kappa^{3/2} t^2} \int_0^{\alpha\omega t} dz \, g(z) \left[ \left( 1 + \left( \frac{z}{\omega\kappa t} \right) \right)^{-3/2} - \left( 1 + \frac{\alpha}{\kappa} \right)^{-3/2} \right] , \tag{39}$$

since the contribution from the lower limit can be shown to be zero for the range of $\omega$ under consideration. This implies the peak contribution to the density comes from those axions emitted just before wall domination.

One can approximate the integrals of $g(z)$ by noting that the dominant contribution comes in the range $4\pi < z < 4\pi n_*$, where $n_*$ is the mode beyond which the radiation spectrum of loops can be truncated due to backreaction. Assuming $4\pi n_* \ll \omega\kappa t$ and $\alpha \lesssim \kappa$, one can use the normalisation condition (36), to deduce that the integral (39) becomes

$$\frac{d\rho_{\rm a}}{d\omega}(t) \approx \frac{4\Gamma_{\rm a} f_{\rm a}^2 \nu}{3\omega\kappa^{3/2}t^2}\left[1-\left(1+\frac{\alpha}{\kappa}\right)^{-3/2}\right]. \tag{40}$$

This estimate is only formally accurate for $\alpha \lesssim \kappa$, but it should also yield useful information for $\alpha \gtrsim \kappa$. From this expression we can obtain the spectral number density of axions

$$\frac{dn_{\rm a}}{d\omega} = \frac{1}{\omega}\frac{d\rho_{\rm a}}{d\omega}. \tag{41}$$

Integrating and comparing with the entropy density of the universe, $s = 2\pi^2\mathcal{N}T^3/45$, the ratio of the axion number density to the entropy at $t_{\rm w}$ can be calculated as

$$\frac{n_{\rm a}}{s} \approx \quad 6.7\times 10^6\left(1+\frac{\kappa}{\alpha}\right)^{3/2}\left[1-\left(1+\frac{\alpha}{\kappa}\right)^{-3/2}\right] \tag{42}$$

$$\Delta\left(\frac{\bar{m}_{\rm a}}{6\times 10^{-6}{\rm eV}}\right)^{-1}\left(\frac{f_{\rm a}}{10^{12}{\rm GeV}}\right)^{2.18}, \tag{43}$$

using typical parameter values $\Gamma_{\rm a} \approx 65$ and $\nu \approx 6\alpha^{1/2}(1+\kappa/\alpha)^{3/2}$. Assuming number conservation after $t_{\rm w}$ and using the entropy density $s_0 = 2809(T_0/2.7{\rm K})^3{\rm cm}^{-3}$ and critical density $\rho_{\rm crit} = 1.88h^2\times 10^{-29}{\rm gcm}^{-3}$ at the present day, one can deduce that the axion loop contribution is

$$\Omega_{{\rm a},\ell} \approx 10.7\left[\left(1+\frac{\alpha}{\kappa}\right)^{3/2}-1\right]h^{-2}\Delta\left(\frac{T_0}{2.7{\rm K}}\right)^3\left(\frac{f_{\rm a}}{10^{12}{\rm GeV}}\right)^{1.18}. \tag{44}$$

It should be noted that the dependence of (44) on the ratio $\alpha/\kappa$ comes about because the lifetime of a loop produced at $t_{\rm i}$ is $(\alpha/\kappa)t_{\rm i}$.

The contribution from long strings can also be roughly estimated assuming that the radiation from the long string network does not affect the scaling balance condition. The basis for this calculation is the radiation power per unit length

$$\frac{dP}{d\ell} \approx \frac{\pi^3 f_{\rm a}^2}{16\gamma t}, \tag{45}$$

with the long string backreaction scale given by $\gamma \sim (\pi^2/8)[\ln(t/\delta)]^{-1}$. Assuming the radiative dominance of this smallest scale $\gamma t$ (as noted elsewhere in simulations[36]), one can calculate the spectral density of axions from long strings

$$\frac{d\rho_{\rm a}}{d\omega} \approx \frac{\pi^3 f_{\rm a}^2 \zeta}{8\gamma\omega t^2}\,. \tag{46}$$

Using similar methods to those used for loops we obtain

$$\Omega_{\rm a,\infty} \approx 1.2 h^{-2} \Delta \left(\frac{T_0}{2.7{\rm K}}\right)^3 \left(\frac{f_{\rm a}}{10^{12}{\rm GeV}}\right)^{1.18}, \tag{47}$$

which is found to be independent of the actual backreaction scale $\gamma$. The considerable uncertainty of (47) must be emphasised given its sensitivity to the amplitude of small-scale structure and the overall long string radiation spectrum. A comparison of the two contributions (44) and (47) yields,

$$\frac{\Omega_{\rm a,\ell}}{\Omega_{\rm a,\infty}} \approx 10.9 \left[\left(1+\frac{\alpha}{\kappa}\right)^{3/2} - 1\right], \tag{48}$$

independent of $\Delta$ and $h$. For the expected parameter range, that is $0.1 < \alpha/\kappa < 1.0$, the loop contribution is considerable larger. We discuss the axion bound quantitatively in the conclusion.

An order-of-magnitude estimate of the demise of the string/domain wall network[37] indicates that there is an additional contribution

$$\Omega_{\rm a,dw} \sim \mathcal{O}(1) h^{-2} \Delta \left(\frac{T_0}{2.7{\rm K}}\right)^3 \left(\frac{f_{\rm a}}{10^{12}{\rm GeV}}\right)^{1.18}. \tag{49}$$

This 'domain wall' contribution is ultimately due to loops which are created at the time $\sim t_{\rm w}$. Although the resulting loop density will be similar to (25), there is not the same accumulation from early times, so it is likely to be subdominant relative to (44). Both the long string and domain wall contributions will serve to strengthen the loop bound (44) on the axion.

## 5 Alternative scenarios

### *5.1 Inflation*

The discussion of the axion density presented so far presumes that a global string network forms after any epoch of inflation, that is, $T_{\rm reh} > f_{\rm a}$ in the standard thermal scenario (i) of section 1.3. In the alternative scenario when

$T_{\rm reh} < f_{\rm a}$, the axion density and any strings formed before inflation are exponentially suppressed by the rapid expansion[d]. In this case, the only contribution to the axion density comes from the initial misalignment mechanism, that is, $\Omega_{\rm a}$ as given by (1). However, $\theta_{\rm i}$ is homogeneous on scales larger then the current horizon and there is no a priori reason to suppose that $\theta_{\rm i}$ should take any particular value. Essentially, with the freedom to choose any value of $\theta_i$, there is no constraint on $f_{\rm a}$. Some authors[16] seem to favour larger values of $\theta_{\rm i} (\sim \pi/2)$ as being more 'natural', since they avoid apparent fine tuning and anthropic arguments about our region of the universe. For example, if one were to chose to conservatively limit $\theta_{\rm i}$ to lie in the range $0.1 \lesssim \theta_{\rm i} \lesssim \pi/2$, then the constraint on the axion becomes $f_{\rm a} \lesssim 10^{11}$–$10^{14}$GeV , ($m_{\rm a} \gtrsim 0.05$–$50\mu$eV), which is—it has to be admitted—a rather indefinite prediction (before other particle physics and cosmological uncertainties are included). Further details about this scenario can be found in general reviews[14].

Various attempts have been made to avoid the anthropic arguments associated with this 'quiescent' inflationary axion by appealing to particle physics-motivated models in which $\theta_{\rm i}$ is set by the conditions at the end of inflation, with one possibility being hybrid inflation[18]. In this case, the axion field is coupled to the inflaton causing the formation of topological defects at the end of inflation, but this returns us to the standard thermal scenario described previously. Such models may occur naturally in supersymmetric axion models[38].

### *5.2 Entropy production*

Entropy production by the out-of-equilibrium decay of massive particles between the QCD phase transition and nucleosynthesis, can weaken all the bounds on $f_{\rm a}$. If the entropy is increased by some factor $\beta$, that is $s \to \beta s$, then the axion density is decreased by a factor $\beta^{-1}$, that is $\Omega_{\rm a} \to \beta^{-1}\Omega_{\rm a}$. For example, it has been noted that that the decay of the saxino—the spin zero partner of the axion—can lead to a dilution by[39]

$$\beta < 5 \times 10^3 \left( \frac{m_{\rm sax}}{1{\rm TeV}} \right), \tag{50}$$

which can be up to a factor of 1000. Such entropy production appears to be a substantial and somewhat inelegant extension of the axion model which

[d]It is possible to form strings during inflation[37], however, the significance of this possibility is far from clear at the present, since quantitative predictions of the initial conditions are difficult to make. If just a small number of long strings survive in the initial distribution, then it may be that the scaling regime can be achieved, albeit slowly. Since the most important axions are those emitted just before the QCD phase transition, the network will have plenty time to reach the appropriate scaling regime.

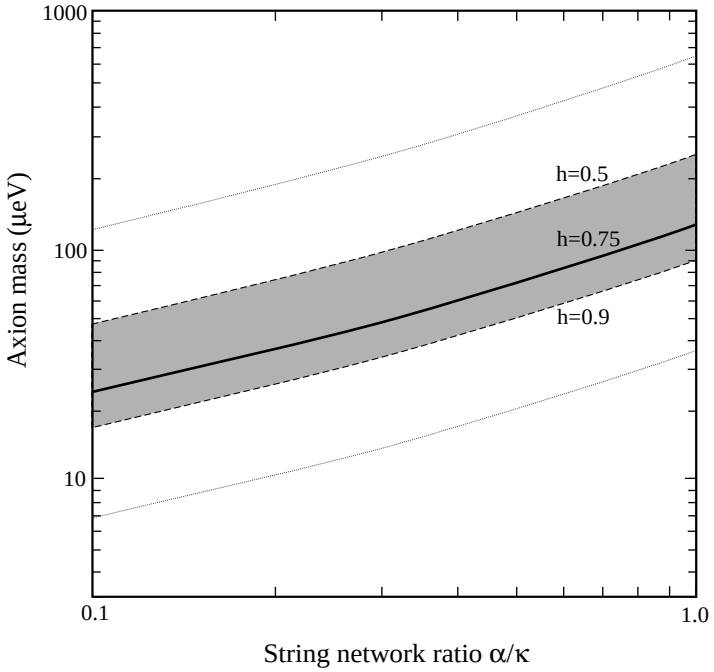


Figure 3: Parameter uncertainties in estimates of the dark matter axion mass. The key string parameter $\alpha/\kappa$ (the loop-size/backreaction-scale ratio) is plotted from the usual assumed value $\alpha/\kappa \approx 1$ to a possible lower limit $\alpha/\kappa = 0.1$. The bold line is the axion mass for a Hubble parameter $h = 0.75$ and the shaded region allows for errors in the range $0.5 \lesssim h \lesssim 0.9$. The dotted line compounds this with particle physics uncertainties.

combines an extra degree of fine-tuning. However, it is another mechanism by which to produce an axion detectable in the current search range 1–10 $\mu$eV.

## 6 Conclusions

The cosmological axion density has been calculated in the standard thermal scenario by considering the dominant contribution from axion strings. Unlike the alternative scenarios described above, there is, in principle, a well-defined calculational method to precisely predict the mass $m_{\rm a}$ of a dark matter axion. For the currently favoured values of the Hubble parameter ($H_0 \approx 75\,{\rm km\,s^{-1}Mpc^{-1}}$), we use string network simulation parameters[27,28] in (44) to

find

$$f_{\rm a} \lesssim 4.7\times10^{10}\,{\rm GeV} \qquad m_{\rm a} \gtrsim 130\,\mu{\rm eV}\,, \qquad h=0.75\,, \tag{51}$$

$$[f_{\rm a} \lesssim 2.3\times10^{10}\,{\rm GeV} \qquad m_{\rm a} \gtrsim 250\,\mu{\rm eV}\,, \qquad h=0.5]\,, \tag{52}$$

$$[f_{\rm a} \lesssim 6.4\times10^{10}\,{\rm GeV} \qquad m_{\rm a} \gtrsim 78\,\mu{\rm eV}\,, \qquad h=0.9]. \tag{53}$$

The key uncertainty in this string calculation is the parameter ratio $\alpha/\kappa$ (that is, the loop-size to backreaction scale ratio). Here, like most authors we have assumed $\alpha/\kappa \approx 1.0$, however, this remains to be firmly established quantitatively. Conceivably, a smaller ratio as low as $\alpha/\kappa \approx 0.1$ is possible and could weaken the bound to $m_{\rm a}\gtrsim 24\,\mu$eV and $f_{\rm a}\lesssim 2.5\times10^{11}$GeV for $h=0.75$. We exhibit the effect of $\alpha/\kappa$ on the axion mass in fig. 3. Reducing this uncertainty remains a key research goal, though a technically difficult one. Also included in fig. 3 are the theoretical particle physics uncertainties, which are about a further factor of 2.5.

Even the weakest axion string bound is considerably stronger than the original constraint from the 'quiescent' production of zero momentum axions for which $f_{\rm a}\lesssim 10^{12}$GeV. This bound narrows the axion window but there still remains a considerable range, $f_{\rm a}\sim 10^9$–$10^{11}$GeV, lying above the astrophysical constraint. These estimates motivate the search for a slightly heavier axion outside the detectable range of the present axion dark matter experiment. Pinpointing more precisely the predicted dark matter axion mass near $m_{\rm a}\sim 100\,\mu$eV remains a theoretical priority.

**Acknowledgments**

EPS is particularly grateful to Professor Klapdor-Kleingrothaus and to the other Heidelberg workshop organisers for their invitation and hospitality. We would both like to thank Alex Vilenkin, Rob Caldwell, Michael Turner, Georg Raffelt and David Lyth for helpful discussions during this work. RAB is supported by PPARC postdoctoral fellowship grant GR/K94799. This work has also been supported by PPARC rolling grant GR/K29272.

## 7 Appendix: Axion string radiation

### *7.1 The Goldstone model*

The essential features of global strings are exhibited in the simple U(1) Goldstone model with action given by

$$S=\int d^4x\left[\partial_\mu\bar\Phi\partial^\mu\Phi-\tfrac{1}{4}\lambda(\bar\Phi\Phi-f_{\rm a}^2)^2\right] \tag{54}$$

$$= \int d^4x \left[ (\partial_\mu \phi)^2 + \phi^2 (\partial_\mu \vartheta)^2 - \tfrac{1}{4}\lambda(\phi^2 - f_{\rm a}^2)^2 \right], \qquad (55)$$

where $\Phi$ is a complex scalar field which has been split as $\Phi = \phi e^{i\vartheta}$ into a massive (real) Higgs component $\phi$ and a massless (real periodic) Goldstone boson $\vartheta$.

For a straight global string in flat space, lying along the $z$-axis, the appropriate ansatz is

$$\Phi(r,\theta) = \phi(r) e^{in\theta}\,, \qquad (56)$$

where $\theta$ is the azimuthal angle and $n$ is the winding number, and one takes the usual boundary conditions, $\phi(0) = 0$ and $\phi \to f_{\rm a}$ as $r \to \infty$. Despite these conditions, the energy per unit length $\mu$ is logarithmically divergent,

$$\mu(\Delta) \;\approx\; \mu_0 + \int_\delta^\Delta \left[ \frac{1}{r} \frac{\partial \Phi}{\partial \theta} \right]^2 2\pi r\, dr \;\approx\; \mu_0 + 2\pi f_{\rm a}^2 \log\left( \frac{\Delta}{\delta} \right), \qquad (57)$$

where $\delta \sim (\sqrt{\lambda}\, f_{\rm a})^{-1}$ is the string core width and $\mu_0 \sim f_{\rm a}^2$ is the core energy associated with the massive field $\phi$ (that is, within $r \lesssim \delta$). The length-scale $\Delta$ is the renormalisation scale provided in general by the curvature radius of the string or the average inter-string separation.

It is clear from this that the string is not localised. However, in the following discussion it will be shown that the dynamics of global strings are similar to those of other types of strings, except for this renormalised string tension. Given $f_{\rm a} \sim 10^{10} - 10^{12}$GeV, the logarithm in (57) implies that there is much more energy in the Goldstone field than in the string core $\mu_0$. Thus the dynamics of the string are dictated by the Goldstone self-field, a fact which has made the understanding of global strings intuitively hazardous.

### *7.2 The Kalb-Ramond Action*

The analytic treatment of global string dynamics is hampered by the topological coupling of the string to the Goldstone boson radiation field. However, we can exploit the well-known duality between a massless scalar field and a two-index antisymmetric tensor field $B_{\mu\nu}$ to replace the Goldstone boson $\vartheta$ in (55) via the relation

$$\phi^2 \partial_\mu \vartheta = \frac{1}{2} f_a \epsilon_{\mu\nu\lambda\rho} \partial^\nu B^{\lambda\rho}\,. \qquad (58)$$

The canonical transformation generated by (58) requires the addition of a total derivative to the action. In this case the total derivative which generates the

transformation is given by[40,41,42]

$$\delta S = \int d^4x\, \epsilon^{\mu\nu\lambda\rho}\partial_\nu B_{\nu\lambda}\partial_\rho\vartheta = \int d^4x\, \epsilon^{\mu\nu\lambda\rho}\Big[\partial_\mu(B_{\nu\lambda}\partial_\rho\vartheta) - B_{\nu\lambda}\partial_\mu\partial_\rho\vartheta\Big] \quad (59)$$

where $\epsilon^{\mu\rho\nu\lambda}$ is the totally antisymmetric tensor in four dimensions. Under this transformation the Goldstone action (55) becomes

$$S = \int d^4x\Big[(\partial_\mu\phi)^2 + \frac{f_a^2}{6\phi^2}H^2 - \frac{1}{4}\lambda(\phi^2 - f_a^2)^2\Big], \quad (60)$$

where the field strength tensor is $H^{\mu\nu\lambda} = \partial^\mu B^{\nu\lambda} + \partial^\lambda B^{\mu\nu} + \partial^\nu B^{\lambda\mu}$. One should note that the sign of the $H^2$ term is the opposite of that one would deduce by substituting the duality relation (58) directly into the Goldstone action (55). One can deduce the correct sign, as shown in (60), by treating the antisymmetric tensor as a Lagrange multiplier.

In the case of a spontaneously broken symmetry, the term added to the action (59) is no longer a total derivative due to the presence of a vortex at $\phi = 0$. One finds that the commutator $\epsilon^{\mu\rho\nu\lambda}\partial_\mu\partial_\rho\vartheta$ is non zero and one can define

$$\epsilon^{\mu\rho\nu\lambda}\partial_\mu\partial_\rho\vartheta = 4\pi J^{\nu\lambda}\,, \quad (61)$$

where $J^{\nu\lambda}$ is an effective current density given by

$$J^{\mu\nu} = \frac{f_{\rm a}}{2}\int \delta^{(4)}\big(x - X(\sigma,\tau)\big)\, d\sigma^{\mu\nu}\,. \quad (62)$$

The area element $d\sigma^{\mu\nu}$ is given in terms of the worldsheet $X(\sigma,\tau)$ swept out by the zeroes of the Higgs field ($\phi = 0$),

$$d\sigma^{\mu\nu} = \epsilon^{ab}\partial_a X^\mu \partial_b X^\nu d\sigma d\tau\,. \quad (63)$$

Rearranging the terms and evaluating the delta function in (61) allows the action to be written as,

$$S = \int d^4x\left[(\partial_\mu\phi)^2 + \frac{f_a^2}{6\phi^2}H^2 - \frac{1}{4}\lambda(\phi^2 - f_a^2)^2\right] - 2\pi f_a\int B_{\mu\nu}d\sigma^{\mu\nu}\,. \quad (64)$$

As for strings for local strings, in the neighbourhood of the string, one may use a local coordinate system to define,

$$x^\mu(\sigma,\tau,\rho^1,\rho^2) = X^\mu(\sigma,\tau) + m_a^\mu\rho^a\,, \quad (65)$$

where $X^\mu(\sigma,\tau)$ are the coordinates on the string worldsheet and $m_a^\mu$ are two orthonormal vectors perpendicular to the worldsheet and $\rho^a$ are related coordinates. If one integrates radially over the massive degrees of freedom by defining the bare string tension to be

$$\mu_0 = -\int d^2\rho \left[ (\partial_\mu \phi)^2 + \frac{1}{6}\left(\frac{f_{\rm a}^2}{\phi^2} - 1\right) H^2 - \frac{1}{4}\lambda(\phi^2 - f_{\rm a}^2)^2 \right], \tag{66}$$

one can deduce the Kalb-Ramond action[43],

$$S = -\mu_0 \int \sqrt{-\gamma}\, d\sigma d\tau + \frac{1}{6}\int d^4x\, H^2 - 2\pi f_a \int B_{\mu\nu} d\sigma^{\mu\nu}\,. \tag{67}$$

where $\gamma_{ab} = g_{\mu\nu}\partial_a X^\mu \partial_b X^\nu$ is the induced metric on the worldsheet and $\gamma = \det(\gamma_{ab})$. The first term is the well known Nambu action of local strings, the second is the antisymmetric tensor field strength for both external fields and the self field of the string and the last is a contact interaction between the $B^{\mu\nu}$ field and the string worldsheet. This coupling between the string and $B_{\mu\nu}$ is analogous to the electromagnetic coupling of a charged particle, and is amenable to the same calculational techniques. This is the basis for the subsequent analytic work reviewed here.

### *7.3 Equations of motion*

Varying the Kalb-Ramond action (67) with respect to the worldsheet coordinates and the antisymmetric tensor, gives the equations of motion for the string and the antisymmetric tensor field equation,

$$\mu_0 \partial_a\big(\sqrt{-\gamma}\gamma^{ab}\partial_b X^\mu\big) = \mathcal{F}^\mu = 2\pi f_{\rm a} H^{\mu\alpha\beta}\epsilon^{ab}\partial_a X_\alpha \partial_b X_\beta\,, \tag{68}$$

$$\partial_\mu H^{\mu\alpha\beta} = -4\pi J^{\alpha\beta} = -2\pi f_{\rm a}\int d\sigma d\tau\, \delta^4\big(x - X(\sigma,\tau)\big)\,\epsilon^{ab}\partial_a X^\alpha \partial_b X^\beta\,. \tag{69}$$

One can use the conformal string gauge $\dot{X}^2 + X'^2 = 0$ and $\dot{X}\cdot X' = 0$, and also the Lorentz gauge of the antisymmetric tensor field, that is, $\partial_\mu B^{\mu\nu} = 0$, to deduce that

$$\mu_0(\ddot{X}^\mu - X''^\mu) = \mathcal{F}^\mu = 2\pi f_a H^{\mu\alpha\beta}(\dot{X}_\alpha X'_\beta - X'_\alpha \dot{X}_\beta)\,, \tag{70}$$

$$\Box B_{\alpha\beta} = 2\pi f_a \int d\sigma d\tau (\dot{X}_\alpha X'_\beta - X'_\alpha \dot{X}_\beta)\delta^{(4)}\big(x - X(\sigma,\tau)\big)\,. \tag{71}$$

As for the point electron one can split up the force $\mathcal{F}^\mu$ into two parts; one due to the self-field and the finite radiation backreaction force. The equations of motion are therefore

$$\mu_0(\ddot{X}^\mu - X''^\mu) = \mathcal{F}^\mu_{\rm s} + \mathcal{F}^\mu_{\rm r}\,, \tag{72}$$

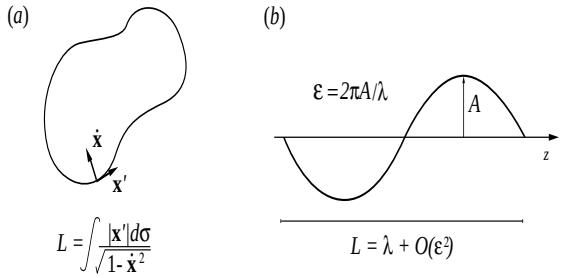


Figure 4: Loop and periodic long string trajectories which have been the subject of extensive analytic and numerical studies.

where the self-force is

$$\mathcal{F}^{\mu}_{\rm s} = -2\pi f_{\rm a}^2 \log(\Delta/\delta)\left[\ddot{X}^{\mu} - X^{\mu\prime\prime}\right] \tag{73}$$

and a first-order approximation to the finite radiation backreaction force is given by[24,19]

$$\mathcal{F}^{\mu}_{\rm r} = \frac{4\pi f_{\rm a}^2 \Delta}{}\left[\dddot{x}^{\mu} - \left(\frac{\dot{X}\cdot\dddot{x}}{\dot{X}^2}\right)\dot{X}^{\mu} + \left(\frac{X'\cdot\dddot{X}}{\dot{X}^2}\right)X^{\mu\prime}\right] . \tag{74}$$

where $\Delta$ is the renormalisation scale introduced in (57). The self field is logarithmically divergent, but it can be absorbed such that the equations of motion in the conformal gauge become[44,45]

$$\mu(\Delta)\big(\ddot{X}^{\mu} - X''^{\mu}\big) = \mathcal{F}^{\mu}_{\rm r} . \tag{75}$$

The renormalised equations of motion (75) for the string can be approximated by the Nambu equations of motion, assuming the effects of radiation backreaction to be small, that is $F^{\mu}_{\rm r} \approx 0$.

These equations have closed loop and periodic long (or infinite) string solutions. The loop solutions are parametrized by their invariant length of the loop $L$, which is closely related to the characteristic frequency $\Omega = 2\pi/L$, whereas the long periodic solutions are parametrized by their wavelength $L$ and the ratio of amplitude to wavelength or the relative amplitude $\mathcal{E} = 2\pi A/L$, where $A$ is their amplitude. Fig. 4 shows a schematic of the two types of solution we have considered in detail.

### *7.4 Appendix conclusion: The nature of string radiation*

The nature of radiation from oscillating axion (and local) strings has been extensively studied[46,42,47,23]. The methods developed allow one, in principle, to calculate the radiation power from any arbitrary periodic loop or long string configurations, yielding the magnitude of the total power as well as the spectrum of the radiation. For arbitrary long string configurations we have also derived a linearized expression which allows one to calculate the leading order contribution to the radiation power[24,19]. By thorough examination of the expressions for the radiation power and applying them to various loop and long string configurations, we have been able to make the following deductions:

(i) The radiation power for loops is independent of the loop size[42,46] with the power given by $P = \Gamma_a f_{\rm a}^2 = \kappa\mu$ which leads to the linear decay in the loop size $\ell = \ell_0 - \kappa(t - t_0)$ as in (33).

(ii) Loops radiate principally in their fundamental mode with a radiation spectrum such that $P_n \propto n^{-q}$ for large $n$ where $q > 4/3$.

(iii) The radiation from long strings is generically in the fundamental mode. However, for exactly periodic solutions the fundamental mode is suppressed and the radiation is quadrupole (as in figs. 1–2).

(iv) The radiation power from long string configurations is proportional to $\mathcal{E}^2$, which leads to the exponential decay of their amplitude $\mathcal{E}$. Again, for exactly periodic configurations cancellation gives radiation proportional to $\mathcal{E}^4$, leading to a power-law type decay.

(v) Some string configurations, like kink solutions, which theoretically have a pathological divergence in their radiation power ($P_n \propto n^{-1}$), rapidly revert to a smooth spectrum dominated by the lowest harmonics because of radiation backreaction effects (see fig. 2).

These predictions broadly uphold the assumptions behind the original work on global string radiation[20,4,5] but they are completely contrary to the predictions of a 'harder' $P_n \propto n^{-1}$ spectrum[30,21,22]. We conclude that axion radiation from axion strings, when extrapolated to cosmological scales, will be very similar to gravitational radiation from Nambu strings.

## References

1. R.D. Peccei and H.R. Quinn, *Phys. Rev. Lett.* **38**, 1440 (1977); *Phys. Rev.* **D16**, 1791.
2. F. Wilczek,, *Phys. Rev. Lett.* **40**, 279 (1978). S. Weinberg, *Phys. Rev. Lett.* **40**, 223 (1978).
3. J. Preskill, M.B. Wise and F. Wilczek, *Phys. Lett.* **120B**, 127 (1983). L. Abbott & P. Sikivie, *Phys. Lett.* **120B**, 133 (1983). M. Dine & W. Fischler, *Phys. Lett.* **120B**, 137 (1983).
4. R.L. Davis, *Phys. Lett.* **180B**, 225 (1986).
5. R.L. Davis and E.P.S. Shellard, *Nucl. Phys.* **B324**, 167 (1989).
6. R.A. Battye and E.P.S Shellard, *Phys. Rev. Lett.* **73**, 2954 (1994). Erratum: *Phys. Rev. Lett.* **76**, 2203.
7. J.L. Rosenberg, *Particle World* **4**, 3 (1995).
8. L.S. Altarev *et al.*, *Phys. Lett.* **276B**, 242 (1992). K.F. Smith *et al.*, *Phys. Lett.* **234B**, 191 (1990).
9. J.E. Moody and F. Wilczek, *Phys. Rev.* **D30**, 130 (1984).
10. D.S.P. Dearbon, D.N Schramm, and G.Steigman, *Phys. Rev. Lett.* **56**, 26 (1986). G.G. Raffelt & D.S.P. Dearborn, *Phys. Rev.* **D36**, 2211 (1987).
11. J. Frieman, S. Dimopoulous and M.S. Turner, *Phys. Rev.* **D36**, 2201 (1987).
12. G. Raffelt [1995], in Proceedings of the XVth Moriond Workshop, *Dark Matter in Cosmology, Clocks and Tests of Fundamental Laws* (see references therein).
13. W. Keil *et al.* [1996], submitted to *Phys. Rev.D* (see references therein)..
14. G.G. Raffelt, *Phys. Rep.* **198**, 1 (1990). M.S. Turner, *Phys. Rep.* **197**, 67 (1990). J.-E. Kim, *Phys. Rep.* **150**, 1 (1987).
15. M.S. Turner, *Phys. Rev.* **D33**, 889 (1986).
16. A.D. Linde, *Phys. Lett.* **201B**, 437 (1988). A.D. Linde, *Phys. Lett.* **259B**, 38 (1991).
17. D.H. Lyth, *Phys. Rev.* **D45**, 3394 (1992).
18. A.D. Linde, *Phys. Lett.* **259B**, 38 (1991).
19. R.A. Battye and E.P.S. Shellard, *Phys. Rev.* **D53**, 1811 (1996).
20. R.L. Davis, *Phys. Rev.* **D32**, 3172 (1985).
21. D.D. Harari and P. Sikivie, *Phys. Lett.* **195B**, 361 (1987).
22. C. Hagmann and P. Sikivie, *Nucl. Phys.* **B363**, 247 (1991).
23. R.A. Battye and E.P.S. Shellard, *Nucl. Phys.* **B423**, 260 (1994).
24. R.A. Battye and E.P.S. Shellard, *Phys. Rev. Lett.* **75**, 4354 (1994).
25. R.A. Battye [1995], PhD thesis (University of Cambridge).
26. A.P. Martin and A.C. Davis, *Nucl. Phys.* **B419**, 341 (1994).
27. D.P. Bennett and F.R. Bouchet, *Phys. Rev.* **D41**, 2408 (1990).
28. B. Allen and E.P.S. Shellard, *Phys. Rev. Lett.* **64**, 119 (1990).

29. P. Sikivie, *Phys. Rev. Lett.* **48**, 1156 (1982).
30. P. Sikivie [1992], 'Dark matter axions', Proceedings of First I.F.T. Workshop on *Dark Matter*, University of Florida, Gainseville, Feb. 14–16, 1992.
31. A. Vilenkin and A.E. Everrett, *Phys. Rev. Lett.* **48**, 1867 (1982).
32. E.P.S. Shellard [1986], in Proceedings of the 26th Liege International Astrophysical Colloquium, *The Origin and Early History of the Universe*, Demaret, J., ed. (University de Liege).
33. E.P.S. Shellard [1990], 'Axion strings and domain walls', in *Formation and Evolution of Cosmic Strings*, Gibbons, G.W., Hawking, S.W., & Vachaspati, V., eds. (Cambridge University Press).
34. W.H. Press, D.N. Spergel, & B.S. Ryden, *Ap. J.* **347**, 590 (1989).
35. A. Vilenkin & E.P.S. Shellard [1994], *Cosmic strings and other Topological Defects* (Cambridge University Press).
36. B. Allen and E.P.S. Shellard, *Phys. Rev.* **D45**, 1898 (1992).
37. D.H. Lyth, *Phys. Lett.* **275B**, 279 (1992).
38. D.H. Lyth and E.D. Stewart, *Phys. Rev.* **D46**, 532 (1992).
39. D.H. Lyth, *Phys. Rev.* **D48**, 4523 (1993).
40. R.L. Davis and E.P.S. Shellard, *Phys. Lett.* **214B**, 219 (1988).
41. E. Witten, *Phys. Lett.* **153B**, 243 (1985).
42. A. Vilenkin and T. Vachaspati, *Phys. Rev.* **D35**, 1138 (1987).
43. M. Kalb and P. Ramond, *Phys. Rev.* **D9**, 2273 (1974).
44. F. Lund and T. Regge, *Phys. Rev.* **D14**, 1525 (1976).
45. A. Dabholkar and J.M. Quashnock, *Nucl. Phys.* **B333**, 815 (1990).
46. T. Vachaspati and A. Vilenkin, *Phys. Rev.* **D31**, 3052 (1985).
47. D. Garfinkle and T. Vachaspati, *Phys. Rev.* **D36**, 2229 (1987). E. Copeland, D.Haws and M.B. Hindmarsh, *Phys. Rev.* **D42**, 726 (1990). M. Sakellariadou, *Phys. Rev.* **D42**, 354 (1990). M. Sakellariadou, *Phys. Rev.* **D44**, 3767 (1991).